



## Review Article

### Corresponding Author

Sung-Hye Park

<https://orcid.org/0000-0002-8681-1597>

Department of Pathology, Seoul National University Hospital, Seoul National University College of Medicine, 101 Daehak-ro, Jongno-gu, Seoul 03080, Korea  
Email: shparknp@snu.ac.kr

Received: March 4, 2022

Revised: May 24, 2022

Accepted: May 25, 2022

# Pathological Classification of the Intramedullary Spinal Cord Tumors According to 2021 World Health Organization Classification of Central Nervous System Tumors, a Single-Institute Experience

Sung-Hye Park<sup>1,2</sup>, Jae Kyung Won<sup>1</sup>, Chi Heon Kim<sup>3</sup>, Ji Hoon Phi<sup>3</sup>, Seung-Ki Kim<sup>3</sup>, Seung Hong Choi<sup>4</sup>, Chun Kee Chung<sup>2</sup>

<sup>1</sup>Department of Pathology, Seoul National University College of Medicine, Seoul, Korea

<sup>2</sup>Institute of Neuroscience, Seoul National University College of Medicine Neuroradiology, Seoul, Korea

<sup>3</sup>Department of Neurosurgery, Seoul National University College of Medicine, Seoul, Korea

<sup>4</sup>Department of Neuroradiology, Seoul National University College of Medicine, Seoul, Korea

According to the new 2021 World Health Organization (WHO) classification of tumors of the central nervous system (CNS) the classification of the primary intramedullary spinal cord tumors (IM-SCT) follows that of CNS tumors. However, since the genetics and methylation profile of ependymal tumors depend on the location of the tumor, the 'spinal (SP)' should be added for the ependymoma (EPN) and subependymoma (SubEPN). For an evidence-based review, the authors reviewed SCTs in the archives of the Seoul National University Hospital over the past decade. The frequent pathologies of primary IM-SCT were SP-EPN (45.1%), hemangioblastoma (20.0%), astrocytic tumors (17.4%, including pilocytic astrocytoma [4.6%] and diffuse midline glioma, H3 K27-altered [4.0%]), myxopapillary EPN (11.0%), and SP-subEPN (3.0%) in decreasing order. *IDH*-mutant astrocytomas, oligodendrogliomas, glioneuronal tumors, embryonal tumors, and germ cell tumors can occur but are extremely rare in the spinal cord. Genetic studies should support for the primary IM-SCT classification. In the 2021 WHO classifications, extramedullary SCT did not change significantly but contained several new genetically defined types of mesenchymal tumors. This article focused on primary IM-SCT for tumor frequency, age, sex difference, pathological features, and genetic abnormalities, based on a single-institute experience.

**Keywords:** Spinal cord, Intramedullary tumor, Ependymoma, Astrocytoma, Diffuse midline glioma



This is an Open Access article distributed under the terms of the Creative Commons Attribution Non-Commercial License (<https://creativecommons.org/licenses/by-nc/4.0/>) which permits unrestricted non-commercial use, distribution, and reproduction in any medium, provided the original work is properly cited.

Copyright © 2022 by the Korean Spinal Neurosurgery Society

## INTRODUCTION

The spinal cord belongs to the central nervous system (CNS) and is a tubular structure that leads to the medulla oblongata, from which any tumor arising from the brain can develop. All intradural extramedullary spinal tumors (EM-SPT) and intramedullary spinal cord tumors (IM-SCT) are rare and account for 2%–4% of CNS tumors.<sup>1</sup> The incidence of spinal cord tu-

mors in Seoul National University Hospital (SNUH) is similar to that reported previously.<sup>2</sup> Reported IM-SCT accounts for approximately about 10% of spinal cord tumors.<sup>1</sup> For the classification of the IM-SCT according to the updated World Health Organization (WHO) classification in 2021, spinal tumors also required genetic studies with some tumors renamed by genetics and methylation profile.<sup>3</sup> The tumor names were changed into spinal ependymoma (SP-EPN) and spinal subependymoma

(SP-subEPN) by adding location, and grades should be written in Arabic rather than Roman characters.<sup>4</sup> Here, authors have summarized the updated knowledge of pathological classification of the primary IM-SCTs.

This article describes an updated classification of IM tumors with frequency, age distribution, sex difference, pathological, and genetic hallmarks according to the 5th edition of WHO classification. Authors reviewed primary spinal cord tumors in the archives of SNUH (Table 1). For the past 10 years (2012–2021), and 329 primary IM-SCTs out of 1,765 cases of both EM- and IM-SCTs were reviewed to determine the above mentioned parameters. Intradural EM-SCT, such as schwannoma, meningioma, neurofibroma, malignant peripheral nerve sheath tumor, solitary fibrous tumor, chordoma, metastatic tumor, and vascular malformation, were excluded. Although genetic studies were not conducted in all SNUH cases, most of the genetic abnormalities screened were meaningful in making a diagnosis or predicting patient's prognosis. Since this article is a case-based review, the authors have added genetic features to the table, but no statistical analysis has been performed. This review of electronic medical records and digital pathology images was approved by the Institutional Review Board of SNUH (IRB No: 2202-097-1301).

Among primary IM tumors at SNUH, spinal ependymomas (SP-EPN) (n = 140, 8.4% of the primary EM- and IM-SCTs and 45.1% of IM-SCT), hemangioblastoma (n = 66, 3.7% of primary spinal tumors and 20.1% of IM-SCT), myxopapillary EPN (2% of primary spinal tumors and 11.0% of IM-SCT), and astrocytic tumors (3.1% of primary spinal tumors, 8.8% of IM-SCT), including low-grade (n = 8, 14% of spinal astrocytic tumors) and high-grade (n = 34, 89.7% of spinal astrocytic tumors), were the most common. The latter high-grade astrocytic tumors included glioblastoma (GBM) IDH-wildtype CNS WHO grade 4 (n = 21, 36.8% of spinal astrocytic tumors) and diffuse midline glioma (DMG) H3 K27M-altered (n = 13, 22.8% of spinal astrocytic tumors). Spinal subEPN (0.6% of primary spinal tumors, 3.0% of the IM-SCT), ganglioglioma (0.3% of primary spinal tumors, 1.5% of IM-SCT), diffuse leptomeningeal glioneuronal tumors (DLGNT), and atypical teratoid/rhabdoid tumor (AT/RT) (0.1% of primary spinal tumors, 0.3% of IM-SCT, each) were rare (Table 1).

The main classification of EM-SPT remains unchanged in the 2021 new WHO classification, but there are newly introduced rare types of CNS mesenchymal tumors, such as intracranial mesenchymal tumor, FET family gene, composed of fused in sarcoma, the Ewing sarcoma, and the TATA-binding

protein-associated factor 2N: cyclic AMP responsive element binding protein 1 (CREB) FET:CREB fusion-positive, capicua transcriptional repressor CIC-rearranged sarcoma, primary intracranial sarcoma, and DICER1-mutant, which can also occur as an EM-SPT.<sup>5-8</sup> In order of increasing frequency, the types of EM-SPT are schwannoma, meningioma, neurofibroma, paraganglioma, chordoma, malignant peripheral nerve sheath tumors, melanocytic tumors, and metastatic tumors.<sup>9</sup> These EM-SPTs are not discussed in this article.

This article summarizes the updated classification of IM-SCTs based on their pathological features and molecular genetic profiles in SNUH cases.

## SPINAL EPENDYMOMAS

SP-EPN is the most common glial tumor of the spinal cord and arises from the ependymal cells of the spinal canal.<sup>10</sup> SP-EPNs were 2.6 times more common (n = 140, 42.7% of IM-SCT) than astrocytic tumors (n = 57, 17.4% of IM-SCT) at SNUH for 10 years from 2012. The incidence of SP-EPNs, myxopapillary EPN, and spinal subEPN comprised 42.7%, 11.0%, and 3.0% of IM-SCT, respectively, at SNUH. The CNS WHO grade 3 SP-EPN was rare, found in 0.5% of primary spinal tumors, 2.4% of IM-SCT, and 5.4% of SP-EPN. The common age for SP-EPN was middle-aged (median, 44 years; range, 2–73 years) with a slight female predominance (male:female ratio 1:1.1) (Table 1). Among the SNUH cases, the most common sites for SP-EPN were at the level of the cervical, lumbar, and thoracic (8:3:1).

SP-EPNs are usually well-circumscribed tumors and have typical perivascular pseudorosettes consisting of a central blood vessel and a surrounding anuclear fibrillary zone (Fig. 1) or true ependymal rosettes with lumina. Tumor cells are monotonous with uniformly round to oval nuclei and salt-and-pepper chromatin. The nucleoli are usually inconspicuous. CNS WHO grade 2 SP-EPNs have a low rate of mitosis rates and a low proliferation index, but necrosis may be present. Rarely, papillary and tancytic subtypes are observed in the spinal cord. Tancytic EPNs favor the spinal cord over the intracranium; however, they were not mentioned in the 2021 WHO classification. Tancytic EPN shows an astrocytoma-like fascicular appearance with indistinct perivascular pseudorosettes, but intratumoral hemorrhage is common (Fig. 2). CNS WHO grade 3 SP-EPNs exhibit high cellularity and brisk mitosis ( $\geq 20/10$  high-power field) with microvascular proliferation, but nuclear pleomorphism is not obvious (Fig. 2). Invasion to the spinal cord parenchyma can occur in CNS WHO grade 3 EPN.

**Table 1.** Epidemiology of the intramedullary spinal cord tumors of SNUH cases, which are listed by their frequency in the spinal cord

Diagnosis	n = 329	% of primary spinal tumors (n = 1,765)	% of IM-spinal tumors (n = 329)	Age (yr), median (range)	Sex, male: female	Known genetics
<b>Ependymal tumors</b>						
SP-EPN, CNS WHO grade 2	140	7.9	42.6	47 (6-73)	1.1:1.	Chromosome 22 deletion (1 copy loss) <i>NF2</i> mutation or deletion
SP-EPN, CNS WHO grade 3	7	0.4	2.1	44 (2-49)	1:2	+ multiple copy number aberration
SP-EPN-MYCN	1	0.1	0.3	49	Female	
Myxopapillary EPN	36	2.0	11.0	40 (15-80)	1.25:1	Unknown
Spinal subEPN	10	0.6	3.0	38 (21-57)	1:1	Unknown
<b>Diffuse adult-type astrocytic tumors</b>						
Astrocytoma, IDH-mutant	0					<i>IDH1/2</i> mutation, <i>ATRX</i> mutation, <i>TP53</i> mutation, <i>CDKN2A/2B</i> homozygous deletion
Oligodendroglioma, IDH-mutant and 1p/19q-codeleted	0					<i>IDH1/2</i> mutation, 1p/19a-codeletion, <i>CIC</i> and/or <i>FUBP1</i> mutation
GBM, IDH-wildtype, CNS WHO grade 4	21	1.2	6.4*	37 (4-59)	1:2	<i>EGFR</i> amplification, <i>PTEN</i> homozygous deletion 7p gain/10 homozygous deletion, <i>TERT</i> promoter mutation, <i>TP53</i> mutation
<b>Diffuse pediatric-type glioma</b>						
Diffuse low-grade glioma	8	0.5	2.4*	37 (1-65)	1.5:1	Unknown
DMG, H3 K27M-altered	13	0.7	4.0*	32.5 (19-75)	1:1.6	<i>H3F3A</i> K27M mutation <i>TP53</i> mutation, <i>ACVR1</i> mutation, <i>ATRX</i> mutation
<b>Circumscribed astrocytic tumors</b>						
Pilocytic astrocytoma, G1	15	0.8	4.6*	37 (1-65)	1:1.2	<i>FGFR1: TACC1</i> fusion, <i>BRAF</i> V600E, <i>KIAA1549-BRAF</i>
<b>Glioneuronal and neuronal tumors</b>						
Ganglioglioma	5	0.3	1.5	5 (2-10)	3:2	<i>KIAA1549-BRAF</i> fusion, <i>NFI</i> mutation, <i>BRAF</i> V600E mutation
Diffuse leptomeningeal glioneuronal tumor	1	0.1	0.3	5 Years	Male	<i>KIAA1549-BRAF</i> fusion, 1p/19 codeletion or 1p deletion or 19q deletion
<b>CNS Embryonal tumor</b>						
Atypical teratoid/rhabdoid tumor	2	0.1	0.6	2 Years	0:1	<i>SMARCB1</i> homozygous deletion or <i>SMCB1</i> mutation
<b>Germ cell tumor</b>						
Germinoma	2	0.1	0.6	22 (the same ages)	0:2	<i>ALK</i> mutation, <i>KIT</i> mutation
Mature cystic teratoma	2	0.1	0.6	28 (0-56)	0:2	<i>KIT</i> mutation, chromosome 12p gain/amplification
<b>Mesenchymal, nonmeningotheelial tumors involving spinal cord</b>						
Hemangioblastoma	66	3.7	20.0	43 (27-76)	2:1	<i>VHL</i> gene mutation

IM, intramedullary; SP-EPN, spinal ependymoma; CNS, central nervous system; WHO, World Health Organization; IDH, isocitrate dehydrogenase; GBM, glioblastoma; DMG, diffuse midline glioma.

\*Total astrocytic tumors including adult-type and pediatric-type diffuse gliomas and pilocytic astrocytoma was 17.4%.



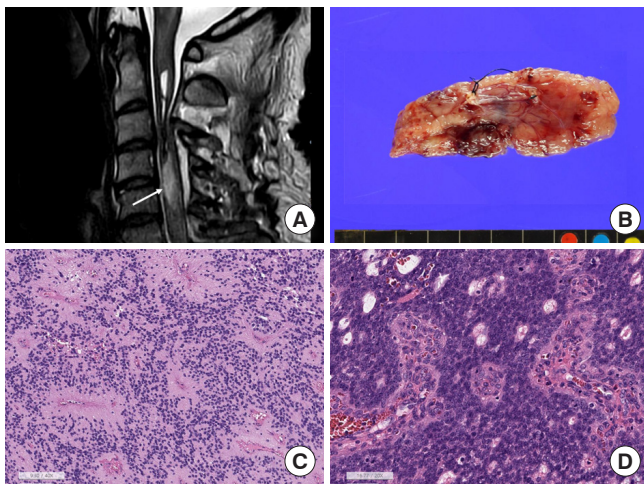


**Fig. 1.** (A) Magnetic resonance imaging shows about 1.7 cm × 0.8 cm × 1.9 cm, mildly enhancing intramedullary mass (arrow) in the C4/5 level with syrinx formation from C2 to C5/6 level with fluid-fluid level, suggestive of hemorrhage and cord edema from C1 to C5 level. (B) Grossly this ependymoma is a well-demarcated finely lobulated tumor. (C) Spinal ependymoma central nervous system (CNS) World Health Organization (WHO) grade 2 shows perivascular pseudorosettes with monotonous small round cells and small round nuclei (H&E; scale, 100 μm). (D) Spinal ependymoma CNS WHO grade 3 reveals high cellular hyperchromatic nuclei with perivascular pseudorosettes and microvascular proliferation (H&E; scale, 100 μm).

All types of EPNs are positive for glial fibrillary acidic protein (GFAP), epithelial membrane antigen (EMA), S100 protein, and vimentin.<sup>11</sup> GFAPs are usually more accentuated in the perivascular anucleated fibrillary zone but diffuse positivity is not uncommon. EMA positivity is represented by a dot-like or tiny ring-like appearance, which is an ultrastructural intracytoplasmic microsette with microvilli and cilia. They are generally negative for oligodendrocyte transcription factor 2 (Olig2) and synaptophysin,<sup>11</sup> and these markers are helpful for the differential diagnosis of astrocytic or neuronal tumors. Since SP-EPN does not show EZHIP overexpression or *H3K27me3* loss in the immunohistochemical study, the presence of these 2 findings should first rule out the drop-down metastasis of posterior fossa group A-EPN. However, *ZFTA-RELA* fusion-positive primary SP-EPN has been reported.<sup>12</sup>

Although SP-EPNs are morphologically similar to supratentorial and posterior fossa EPNs, the molecular genetics and methylation profiles of these SP-EPNs are different from those of intracranial EPNs.<sup>13,14</sup> The most common genetic abnormalities of SP-EPNs are one copy loss of *NF2* or *NF2* mutations.<sup>11,15,16</sup> CNS WHO grade 3 EPNs commonly have multiple chromo-

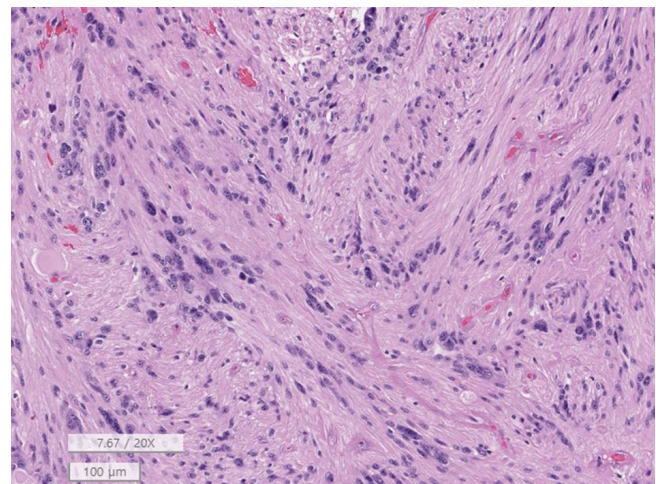


**Fig. 2.** Tanycytic ependymoma shows a fascicular pattern of the tumor with fibrillary cytoplasm of tumor cells and indistinct ependymal rosettes, morphologically indistinct from astrocytic tumors (H&E; scale, 100 μm).

somal copy number aberrations, in addition to one copy loss of *NF2* or *NF2* mutations. According to Lee et al.<sup>17</sup> the frequency of *NF2* mutations in spinal and intracranial EPN was 32.1 and 4.4%, respectively.

*MYCN* gene amplified SP-EPN (SP-EPN-*MYCN*) has been recognized as a rare subtype of SP-EPN characterized by multiple tumors and aggressive behavior.<sup>18</sup> This SP-EPN-*MYCN* has histopathological features of high-grade ependymoma, such as high cellularity, microvascular proliferation, brisk mitosis, tumor necrosis, and high MIB-1 proliferation index. Robust nuclear *MYCN* expression or in situ hybridization with the *MYCN*-locus probe may be useful for detecting *MYCN* amplification, as well as NGS studies (Fig. 1D).

## MYXOPAPILLARY EPENDYMOMAS

Myxopapillary EPNs, CNS WHO grade 2, are not uncommon, constituting approximately 11% of IM-SCTs in SNUH. These tumors commonly occur at the distal thoracic to lumbar region (T12 to L2, 3), including the sacrum and filum terminale, but rarely at the upper thoracic or cervical levels of the spinal cord.<sup>19</sup> The median age of SNUH patients with myxopapillary EPNs was 40 years (range, 15–80 years). Grossly, these tumors are well-encapsulated and often dumbbell-shaped solid masses composed of hyalinized blood vessels and a myxoid or mucinous intercellular matrix. The tumor cells show a monotonous polygonal appearance but sometimes long bipolar fibrillary cytoplasmic processes. The nuclei are usually round to oval and

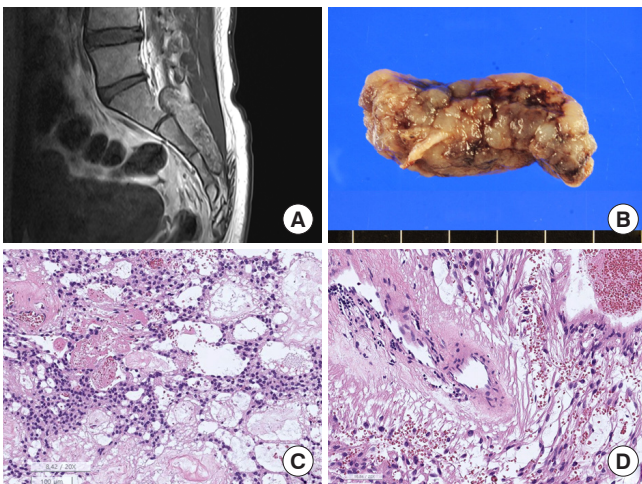


**Fig. 3.** Myxopapillary ependymoma. (A) Magnetic resonance imaging. A 6.1 cm × 1.8 cm × 7.8 cm, T2 heterogeneous hyperintense and hypointense extradural (epidural) soft tissue mass in the S1–3 sacral central canal. There are multifocal pressure bone erosion and resultant central canal widening. (B) The tumor shows a well-demarcated and multilobulated appearance. (C) The tumor shows sheets of polygonal cells with a lake of myxoid and mucinous material and hemorrhage and fibrinous material (H&E; scale, 100 µm). (D) The vascular wall is hyalinized and tumor cells have long fibrillary cytoplasmic processes (H&E; scale, 50 µm).

bland-looking, but sometimes enlarged nuclei is present due to degenerating atypia (Fig. 3). These tumors have a favorable prognosis with 10-year overall survival rates > 90%.<sup>20</sup> Myxopapillary EPNs rarely metastasize to extraneural sites.<sup>21</sup>

## SUBEPENDYMOMA

SubEPNs are rare primary benign IM-SCTs classified as CNS WHO grade 1 tumors. In SNUH, they account for 0.6% of SPT and 3.0% of IM-SCT and usually occurred between 20 and 60 years (median, 38 years; range, 21–57 years). They commonly occur at cervical and thoracic levels. SP-subEPNs are well-circumscribed or well-encapsulated tumors that show typical microscopic features, including alternative cellular and acellular areas with microrosette-like multiple cell aggregates (Fig. 4). Metastases are extremely rare, and neither necrosis nor spinal cord invasion are observed. Degenerative nuclear atypia is rarely found, but is not a high-grade feature. Occasionally, in otherwise typical cases, fibrillary astroglial or gemistocytic cells may appear (Fig. 4). Immunohistochemical findings are similar to those of EPN; thus, GFAP is diffusely positive and might exhibit focal dot-like positivity for EMA, but negative for synap-

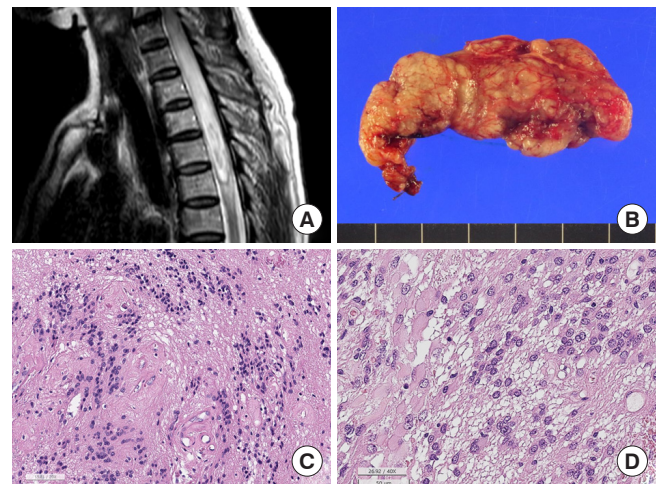


**Fig. 4.** Subependymoma. (A) Magnetic resonance imaging. Diffuse intramedullary T2 hyperintensity lesion with swelling of the spinal cord, C6–T5 level, and focal enhancement. (B) Resected tumor shows well-demarcated lobulated yellow tan-colored tumor. (C) Histopathologically alternative cellular and acellular areas with nuclear aggregates (H&E; scale, 50 µm). (D) Some ependymomas show gemistocytes-like plump eosinophilic cytoplasm (H&E; scale, 50 µm).

physin and Olig2. Although little is known about the genetic alterations in subEPN, mutations in the *TRSI* gene have been found in familial subEPNs.<sup>22</sup> *BRAF* and *H3F3A* mutations are absent and *H3K27me3* is retained in the tumor cells. Spinal subEPNs are also morphologically identical to intracranial subEPNs; however, the methylation profile of spinal subEPN is different from that of intracranial and posterior fossa subEPN. Even after partial resection, the prognosis is excellent, and recurrence after surgery is rare.<sup>23</sup>

## DIFFUSE ASTROCYTIC TUMORS, INCLUDING ADULT-TYPE DIFFUSE GLIOMAS AND PEDIATRIC-TYPE DIFFUSE GLIOMAS

Astrocytomas constituted 17.4% of IM-SCT, including diffuse astrocytoma (n = 29, including 8 low- and 21 high-grade astrocytomas), DMG H3K27-altered (n = 13), and pilocytic astrocytoma (n = 15). Pilocytic astrocytoma, CNS WHO grade 1 was found in 4.6% of IM-SCT, diffuse low-grade gliomas (2.4% of IM-SCT), and diffuse high-grade glioma (DHGG, 10.4% of IM-SCT). In SNUH cases, GBM IDH-wildtype (6.4% of IM-SCT) and DMG H3 K27M-altered (4.0% of IM-SCT) were the most common malignant astrocytic tumors (DHGG).

According to Hamilton et al.<sup>24</sup> only 13% of spinal gliomas,



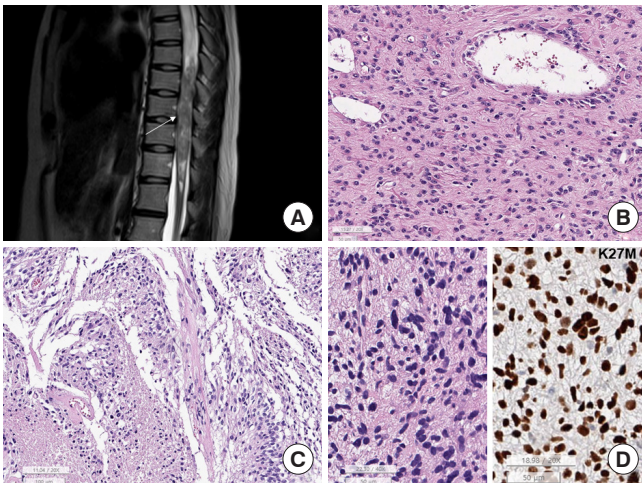


**Fig. 5.** Spinal astrocytoma. (A) Magnetic resonance imaging. Intramedullary glioblastoma shows T2 heterogeneous mass (arrow) at T7–12 levels with multifocal enhancement and is associated with syrinx from C4 to T7 level. (B) The low-grade astrocytic tumor shows sheets of astrocytic cells with eosinophilic cytoplasm (H&E; scale, 50  $\mu$ m). (C) The highly cellular tumor has multiple foci of necrosis (asterisk) with pseudopalisading nuclei (H&E; scale, 100  $\mu$ m). (D) Diffuse midline glioma shows sheets of hyperchromatic elongated cells. Left: the tumor cells of DMG, H3K27-altered are arranged in sheet with elongated nuclei, looked like astrocytic tumor (H&E of DMG H3K27-altered; scale, 50  $\mu$ m); right: the tumor cell nuclei of DMG are positive for K27M (K27M immunohistochemistry; scale, 50  $\mu$ m).

including pediatric gliomas, was malignant. As the histopathology of spinal astrocytic tumors is similar to that of intracranial astrocytic tumors (Fig. 5), low grade gliomas (LGGs) have scant mitoses, no microvascular proliferation, no necrosis and low Ki-67 labeling index (Fig. 5B). GBM usually had pleomorphic nuclei of tumor cells, microvascular proliferation, and/or necrosis (Fig. 5A, C).

The genetics of spinal LGG is not well known because they are rare, but *BRAF* gene alterations have been reported.<sup>25</sup> Most spinal GBMs were IDH-wildtype de novo tumors with *EGFR* amplification and/or *PTEN* or *CDKN2A* homozygous deletion, and *TERT* promoter and/or *TP53* mutations have been found in the SNUH series, which is similar to the cases of Nagaiishi et al.<sup>26</sup>

Although several cases of spinal *IDH*-mutant astrocytomas and spinal oligodendrogliomas have been reported, they are extremely rare.<sup>27,28</sup> Hemispheric gliomas, such as diffuse hemispheric glioma, *H3* G34-mutant, and infant-type hemispheric glioma, are also extremely rare.

DMG, H3 K27-altered in the spinal cord, is a relatively re-

cently recognized aggressive glioma classified as CNS WHO grade 4.<sup>29</sup> Since the median age of DMG H3 K27-altered was 32.5 years old (range, 19–75 years old) in SNUH cases, spinal DMG can occur at any age and is more common in adults. These tumors carry somatic mutations of *H3F3A* or *HIST1H3B/C*.<sup>29</sup> Morphologically, DMG can have various grades of astrocytic tumors (Fig. 5D); therefore, it can appear as low-grade astrocytoma or typical GBM, or have a primitive neuroectodermal tumor-like appearance. The tumor cells were positive for GFAP, and the tumor cell nuclei were positive for the H3K27M-mutant specific antibody, K27M (Fig. 5D). However, spinal cord DMG H3 K27-altered has a slightly better prognosis than spinal GBM, CNS WHO grade 4.<sup>30</sup> *TP53*, *ATRX*, and *ACVR1* mutations commonly accompany these tumors.<sup>31</sup> However, *EGFR*-mutant DMG, known as bithalamic glioma, and *EZH2*-overexpressing spinal DMG have never been reported in the spinal cord.

## CIRCUMSCRIBED ASTROCYTIC GLIOMAS

Pilocytic astrocytoma is a relatively well-circumscribed and indolent CNS WHO grade 1 astrocytoma. Although pilocytic astrocytoma commonly occurs in the posterior fossa and optic pathway in children and adolescents, spinal pilocytic astrocytoma accounted for 4.3% of all IM-spinal tumors at SNUH (Table 1). The age of onset of spinal pilocytic astrocytomas was slightly higher (median, 37 years; range, 1–65 years) than that of supratentorial tumors.

The histopathology of spinal pilocytic astrocytoma is similar to that of intracranial pilocytic astrocytoma, showing low cellularity and bland-looking elongated nuclei with bipolar cytoplasmic processes. Vascular hyalinization and Rosenthal fibers are common (Fig. 6). Occasionally, degenerative nuclear atypia is observed.

Ninety percent of posterior fossa-pilocytic astrocytomas and 60% of optic pathway-pilocytic astrocytomas are known to have *KIAA1549:BRAF* fusion, and the remaining cases have mitogen-activated protein kinase (MAPK) pathway gene alterations, including *BRAF V600E*, *NF1*, *PTPN11*, and *FGFR1* mutations.<sup>32</sup> Although 40% of spinal pilocytic astrocytomas have *KIAA1549:BRAF* fusion, *BRAF V600E* mutation has been found in 4% of spinal pilocytic astrocytomas. Furthermore, homozygous deletion of *CDKN2A* is slightly more common in spinal cord and brainstem pilocytic astrocytoma than in cerebellar ones (21.1% vs. 33.3%).<sup>33</sup> *FGFR1:TACC1* fusion has been reported in pilo-

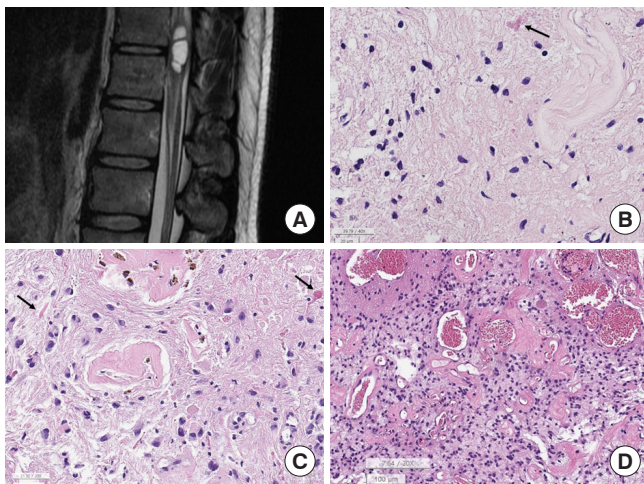


**Fig. 6.** Spinal pilocytic astrocytoma, 3 cases with various histology. (A) Magnetic resonance imaging. About 3.2-cm-sized dorsally exophytic intramedullary tumor at the C1–2 level and shows T2 high signal intensity. (B) The tumor shows low cellularity, a hyalinized blood vessel, and a Rosenthal fiber (arrow) (H&E; scale, 20  $\mu$ m). (C) Another pilocytic astrocytoma shows nuclear pleomorphism which is degenerated nuclear atypia with hyalinized blood vessels and Rosenthal fibers (arrows) (H&E; scale, 50  $\mu$ m). (D) The other pilocytic astrocytoma shows moderately cellularity with ectatic and congested blood vessels and hyalinized vascular wall (H&E; scale, 100  $\mu$ m).

cytic astrocytoma occurring in the brainstem and near full-length of the cervical spinal cord of a 22-year-old female.<sup>34</sup> One of our spinal pilocytic astrocytomas in a 65-year-old male had an *FGFR1:TAC1* fusion.

Other circumscribed astrocytic gliomas, such as high-grade astrocytoma with piloid features, pleomorphic xanthoastrocytoma, and MN1-altered astroblastoma, rarely occur in the IM-spinal cord; however, subependymal giant cell astrocytoma and chordoid glioma have never been reported in the spinal cord.<sup>35–38</sup>

## GLIONEURONAL AND NEURONAL TUMORS

Ganglioglioma, CNS WHO grade 1 was the most common glioma, accounting for 1.5% of primary IM-SCT in SNUH. DLGNT rarely occurred in the spinal cord (0.3% of IM-SCT).

Ganglioglioma is a relatively well-demarcated, slow-growing neoplasm of childhood. The median age of patients with ganglioma was 5 years old (range, 2–10 years) in SNUH. Sometimes, they involve the long segments of the spinal cord.<sup>39</sup> Gangliogliomas are composed of 2 cell components, neoplastic ganglion cells and glial cells (Fig. 7). These tumors are usually caused

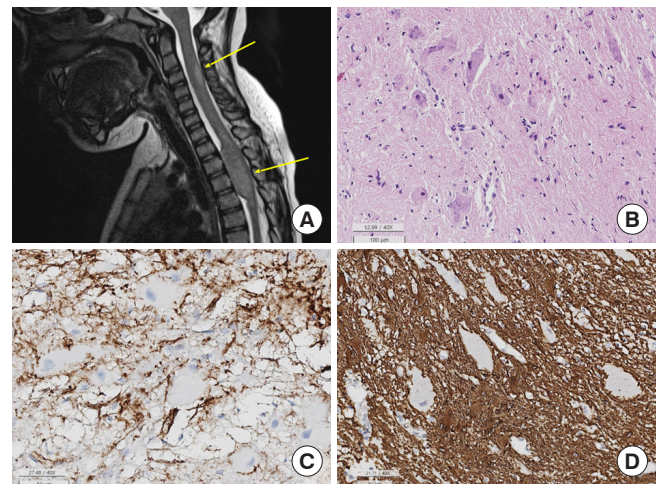


**Fig. 7.** Spinal ganglioglioma. (A) Magnetic resonance imaging reveals intramedullary, bulging mass (arrows) involving C6–T5 spinal cord - eccentric location and T2 high SI with partial enhancement. (B) The tumor is composed of mature ganglion cells and glial cells (H&E; scale, 100  $\mu$ m). (C) The glial cells are positive for CD34 but ganglion cells are negative for CD34 (scale, 50  $\mu$ m). (D) The glial cells are positive for glial fibrillary acidic protein (GFAP), but ganglion cells are negative for GFAP (50  $\mu$ m).

by alterations in the MAPK signaling pathway, usually with a *KIAA1549:BRAF* fusion; however, *BRAF* V600E and *NF1* (sometimes biallelic) mutations or deletions have also been observed. Very rarely, spinal gangliogliomas contain only *H3K27M* mutations.

DLGNT is a low-grade glioneuronal neoplasm characterized by widespread diffuse involvement of the leptomeninges and superficial brain parenchyma by monotonous oligodendroglioma-like cells with bidirectional differentiation.<sup>40</sup> These tumors are commonly found in the subpial region of the basal surface of the brain, brainstem, and spinal cord. Genetically, *KIAA1549:BRAF* fusion was found in 72% of the studied cases while 1p and/or 19q deletion was found in other cases.<sup>41</sup> 1p/19q codeletion has been identified in 18%–33%.<sup>41,42</sup> Based on the methylation profiles, these tumors are classified into methylation classes 1 and 2 (MC1 and MC2). Although MC1 is roughly similar to CNS WHO grade 2 gliomas in clinical course, MC2 has anaplastic features, 1q gain, and/or a worse prognosis than MC1.<sup>43</sup>

## CNS EMBRYONAL TUMORS

Among embryonal tumors, AT/RT, CNS WHO grade 4, rarely occur in the IM-spinal cord of infants (0.6% of IM-SCT), while other embryonal tumors are extremely rare. Approximately 7.6%



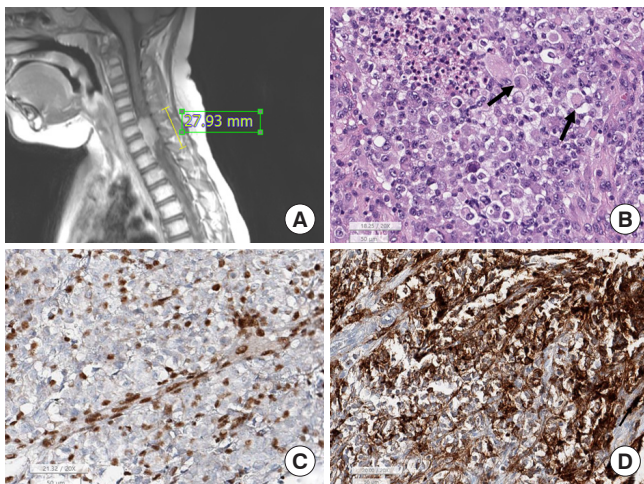


**Fig. 8.** Atypical teratoid rhabdoid tumor. (A) Magnetic resonance imaging shows a 2.8-cm elongated epidural enhancing mass between C5 and T1. (B) Light microscopically the tumor shows small round cells with eccentrically located nuclei and eosinophilic cytoplasm (arrows), which is a rhabdoid feature. (C) The tumor cell nuclei are negative for INI-1, but include internal control, such as endothelial cells and some inflammatory cells are positive for INI-1 (INI-1 immunohistochemistry; scale, 50  $\mu$ m). (D) The tumor cells are at least focal positive for epithelial membrane antigen (EMA; scale, 50  $\mu$ m).

of AT/RT occurs in the spinal cord.<sup>44</sup> If this tumor develops in the EM-spinal cord, i.e., extradural or paravertebral, or in patients aged 3 years or older, metastasis of extracranial malignant rhabdoid tumor should be ruled out first. The pathological and genetic features were identical to those of intracranial AT/RT in SNUH. The tumor presents as a monotonous small round cell tumor with an eccentric nucleus and a prominent eosinophilic rhabdoid appearance, but primitive small round cells with scanty cytoplasm can be seen (Fig. 8). Tumor cell nuclei are usually negative for INI-1 and the Ki-67 labeling index is usually very high. *SMARCB1* mutations or homozygous deletions are the genetic hallmarks of this tumor.<sup>45</sup> Since poorly differentiated chordomas also have *SMARCB1*/INI-1 loss, pathologists should keep it in mind when making a differential diagnosis.<sup>46</sup> Biological behavior is as aggressive as intracranial AT/RT.<sup>45</sup>

## GERM CELL TUMORS

Mature cystic teratomas, immature teratomas, and pure germinomas can occur in the spinal cord. In the SNUH series, these germ cell tumors are extremely rare, with each tumor subtype occurring in 0.1% of SPT and 0.6% of IM-SCT. Germinoma occurred in T12–L1 and young adults, and interestingly, 2 cases

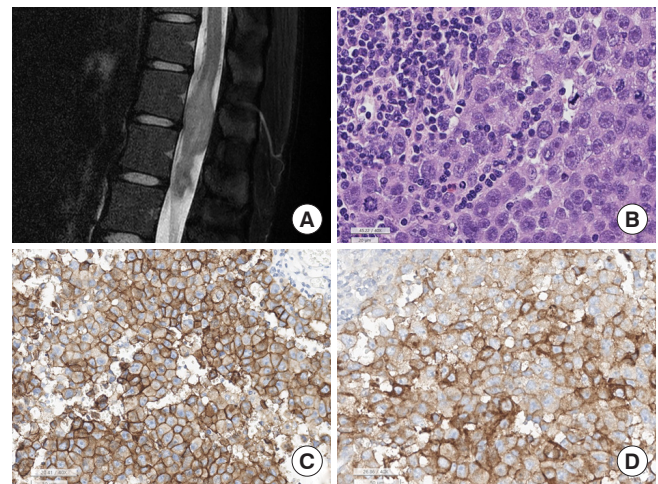


**Fig. 9.** Germinoma. (A) Magnetic resonance imaging shows T2 heterogeneous intensity mass at T12–L1 spinal cord, involving conus medullaris. (B) The tumor is composed of biphasic, malignant germ cells and lymphoplasmic cells (H&E; scale, 20  $\mu$ m). The malignant germ cells show large round nuclei and prominent nucleoli. There are frequent mitoses. (C) The tumor cell membrane is positive for c-kit (scale, 50  $\mu$ m), and (D) placental alkaline phosphatase (PLAP; scale, 50  $\mu$ m).

of SNUH germinoma occurred in 22-year-old females. Teratomas also commonly arise in the lower spinal level from L2 to the coccyx at any age. The 2 SNUH teratomas occurred in an infant and a 56-year-old woman. The histopathology of spinal teratomas and germinomas is identical to that of extraspinal tumors. Pure germinomas consist of malignant germ cells and lymphoplasmic cells. Malignant germ cells are arranged in sheets of polygonal-shaped malignant germ cells, which have centrally located rounded nuclei and prominent nucleoli (Fig. 9). The cytoplasm is moderate to plump and shows a pink to clear appearance because of the large amount of glycogen and lipid vacuoles. High rates of mitosis and necrosis are also common. Characteristically, germinoma cells have a positive membranous expression of c-kit and are commonly positive for placental alkaline phosphatase. Mature teratomas have mature 3-germ-layer tissues. Immature teratomas contain primitive neuroepithelial tubules. Genetically, one germinoma of SNUH cases had an *ALK* gene mutation (p.Gly926fs, c.2775delAinsGG); in addition, *KIT* mutation and chromosome 12p gain or amplification have been reported in intracranial germ cell tumors.<sup>47</sup>

## HEMANGIOBLASTOMAS

Hemangioblastoma, CNS WHO grade 1, is the second most common IM-SCT after ependymomas, accounting for 3.7% of



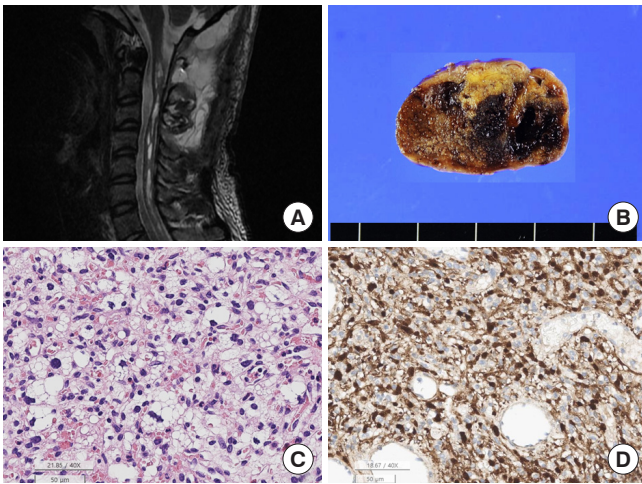


**Fig. 10.** Hemangioblastoma. (A) Magnetic resonance imaging shows a 5.1-cm solid and cystic tumor with multifocal enhancement in at C2–T3 Spinal cord with a tiny intramedullary enhancing nodule at C2–T3 levels with spinal cord edema. (B) The tumor shows a well-demarcated hemorrhage mass. (C) The tumor is highly vascular with rich capillaries. The tumor cells have round to mildly pleomorphic nuclei and foamy cytoplasm (H&E; scale, 50  $\mu$ m). (D) The nuclei and cytoplasm of the tumor cells are positive for S-100 protein, but the capillary endothelial cells are negative for S-100 protein (S-100 immunohistochemistry; scale, 50  $\mu$ m).

all primary SPT and approximately 20.0% of IM-SCT in SNUH. Hemangioblastomas do not undergo malignant transformations. However, both IM and EM hemangioblastomas have been reported.<sup>48,49</sup> In SNUH cases, hemangioblastoma was 1.5 times more common than astrocytic tumors and 1/3 less common than SP-EPN. Hemangioblastomas are adult tumors that occur in a wide range of patients (mean age, 43 years; range, 16–81 years). The male to female ratio was 2:1. Hemangioblastomas occur at any level from the cervical spine to the lumbar spinal cord. The tumors are well-circumscribed, pseudoencapsulated, and capillary-rich solid tumors. The tumor cells are stromal cells with foamy cytoplasm, and the capillaries are nonneoplastic components (Fig. 10). Ultrastructurally, tumor cells have many cytoplasmic fat vacuoles and intermediate filaments, which produce foamy cytoplasm on H&E staining. Tumor cells express NSE, S100, alpha-inhibin, D2-40, and brachyury (cytoplasmic expression), which can help in the differential diagnosis.<sup>50</sup> The pathogenesis and cells of origin remain unknown. In rare cases, hyaline globules are present. This tumor may be sporadic or be associated with von Hippel-Lindau disease. However, the tumor usually has various kinds of *VHL* gene mutations, such as missense, slicing, insertion, or deletion mutations.<sup>51,52</sup>

When the tumor is completely removed, the prognosis is good.<sup>53</sup>

## CONCLUSION

Theoretically, any type of primary CNS tumor can occur in the intramedullary spinal cord; however, the most common IM-SCT is EPN, followed by hemangioblastoma and astrocytoma. SP-EPN and SP-subEPN are morphologically identical to those of the supratentorial or posterior fossa, but their molecular genetic and methylation profiles differ from those of intracranial EPN. Therefore, these tumors should have ‘spinal’ in the tumor name. DLGNT can arise in the spinal cord and are characterized by a *KIAA1549:BRAF* fusion, 1p and/or 19q deletion, or 19q gain. In addition, some spinal pilocytic astrocytomas are characterized by *FGFR1:TACC1* fusion, in addition to alterations in the MAPK pathway. Myxopapillary ependymomas characteristically occur in the lumbosacral area and are regarded as CNS WHO grade 2.<sup>4</sup> Although spinal DMG H3 K27M-altered is a high-grade glioma, the biological behavior of spinal DMG is better than that of spinal GBM IDH-wildtype, CNS WHO grade 4. Rarely, pilocytic astrocytoma, ganglioglioma, diffuse leptomeningeal glioma, and atypical teratoid rhabdoid tumors occur in IM-SCT; they may share a *KIAA1549:BRAF* fusion. However, although several cases of spinal *IDH*-mutant astrocytomas have been reported, hemispheric gliomas (such as diffuse hemispheric glioma, H3 G34-mutant, and infant-type hemispheric glioma) or *IDH*-mutant gliomas (including *IDH*-mutant astrocytoma and oligodendroglioma) are extremely rare.

## NOTES

**Ethics Statement:** The institutional review board of our hospital approved this study (IRB No: 2202-097-1301) and has therefore been performed under the ethical standards set out in the 1964 Declaration of Helsinki and its subsequent amendments. As this study is a retrospective review of anonymized electronic medical records, pathology, and results of NGS data utilizing a brain tumor-specific somatic gene panel, informed consent was waived from our IRB under the Korean Bioethics and Safety Act. All materials had been obtained for the electronic medical record of the patients, which were anonymized and retrospectively reviewed. No extra-human materials were obtained from the patients for this study. Under the Korean Bioethics and Safety Act, additional consent to publish was waived.

**Conflict of Interest:** The authors have nothing to disclose.

**Funding/Support:** This study was supported by a grant from

the Korea Health Technology R&D Project through the Korea Health Industry Development Institute (KHIDI), funded by the Ministry of Health & Welfare, Republic of Korea (grant number: HI14C1277).

**Author Contribution:** Conceptualization: SP; Data curation: JKW, CHK, JHP, SK, SC, CKC; Writing - original draft: SP; Writing - review & editing: SP

## ORCID

Sung-Hye Park: 0000-0002-8681-1597

Jae Kyung Won: 0000-0003-1459-8093

Chi Heon Kim: 0000-0003-0497-1130

Ji Hoon Phi: 0000-0002-9603-5843

Seung-Ki Kim: 0000-0002-0039-0083

Seung-Hong Choi: 0000-0002-0412-2270

Chun Kee Chung: 0000-0003-3485-2327

## REFERENCES

1. Abd-El-Barr MM, Huang KT, Moses ZB, et al. Recent advances in intradural spinal tumors. *Neuro Oncol* 2018;20:729-42.
2. Chamberlain MC, Tredway TL. Adult primary intradural spinal cord tumors: a review. *Curr Neurol Neurosci Rep* 2011;11:320-8.
3. Witt H, Gramatzki D, Hentschel B, et al. DNA methylation-based classification of ependymomas in adulthood: implications for diagnosis and treatment. *Neuro Oncol* 2018;20:1616-24.
4. Louis DN, Perry A, Wesseling P, et al. The 2021 WHO Classification of Tumors of the Central Nervous System: a summary. *Neuro Oncol* 2021;23:1231-51.
5. Sloan EA, Chiang J, Villanueva-Meyer JE, et al. Intracranial mesenchymal tumor with FET-CREB fusion-A unifying diagnosis for the spectrum of intracranial myxoid mesenchymal tumors and angiomatoid fibrous histiocytoma-like neoplasms. *Brain Pathol* 2021;31:e12918.
6. Alexandrescu S, Meredith DM, Lidov HG, et al. Loss of histone H3 trimethylation on lysine 27 and nuclear expression of transducin-like enhancer 1 in primary intracranial sarcoma, DICER1-mutant. *Histopathology* 2021;78:265-75.
7. Sakaguchi M, Nakano Y, Honda-Kitahara M, et al. Two cases of primary supratentorial intracranial rhabdomyosarcoma with DICER1 mutation which may belong to a "spindle cell sarcoma with rhabdomyosarcoma-like feature, DICER1 mutant". *Brain Tumor Pathol* 2019;36:174-82.
8. Yang S, Liu L, Yan Y, et al. CIC-NUTM1 sarcomas affecting the spine. *Arch Pathol Lab Med* 2022;146:735-41.
9. Koeller KK, Shih RY. Intradural extramedullary spinal neoplasms: radiologic-pathologic correlation. *Radiographics* 2019;39:468-90.
10. Lamszus K, Lachenmayer L, Heinemann U, et al. Molecular genetic alterations on chromosomes 11 and 22 in ependymomas. *Int J Cancer* 2001;91:803-8.
11. Leeper H, Felicella MM, Walbert T. Recent advances in the classification and treatment of ependymomas. *Curr Treat Options Oncol* 2017;18:55.
12. Lim KY, Lee KH, Phi JH, et al. ZFTA-YAP1 fusion-positive ependymoma can occur in the spinal cord: Letter to the editor. *Brain Pathol* 2022;32:e13020.
13. Cho HJ, Park HY, Kim K, et al. Methylation and molecular profiles of ependymoma: influence of patient age and tumor anatomic location. *Mol Clin Oncol* 2021;14:88.
14. Ahmad O, Chapman R, Storer LC, et al. Integrative molecular characterization of pediatric spinal ependymoma: the UK Children's Cancer and Leukaemia Group study. *Neurooncol Adv* 2021;3:vdab043.
15. Zemmoura I, Vourc'h P, Paubel A, et al. A deletion causing NF2 exon 9 skipping is associated with familial autosomal dominant intramedullary ependymoma. *Neuro Oncol* 2014;16:250-5.
16. Lim KY, Lee K, Shim Y, et al. Molecular subtyping of ependymoma and prognostic impact of Ki-67. *Brain Tumor Pathol* 2022;39:1-13.
17. Lee CH, Chung CK, Kim CH. Genetic differences on intracranial versus spinal cord ependymal tumors: a meta-analysis of genetic researches. *Eur Spine J* 2016;25:3942-51.
18. Ghasemi DR, Sill M, Okonechnikov K, et al. MYCN amplification drives an aggressive form of spinal ependymoma. *Acta Neuropathol* 2019;138:1075-89.
19. Acerbi F, Vetrano IG, Sattin T, et al. The role of indocyanine green videoangiography with FLOW 800 analysis for the surgical management of central nervous system tumors: an update. *Neurosurg Focus* 2018;44:E6.
20. Abdallah A, Emel E, Gunduz HB, et al. Long-term surgical resection outcomes of pediatric myxopapillary ependymoma: experience of two centers and brief literature review. *World Neurosurg* 2020;136:e245-61.
21. Fujimori T, Iwasaki M, Nagamoto Y, et al. Extraneural metastasis of ependymoma in the cauda equina. *Global Spine J* 2013;3:33-40.
22. Fischer SB, Attenhofer M, Gultekin SH, et al. TRPS1 gene



- alterations in human subependymoma. *J Neurooncol* 2017; 134:133-8.
23. Yuh WT, Chung CK, Park SH, et al. Spinal cord subependymoma surgery: a multi-institutional experience. *J Korean Neurosurg Soc* 2018;61:233-42.
  24. Hamilton KR, Lee SS, Urquhart JC, et al. A systematic review of outcome in intramedullary ependymoma and astrocytoma. *J Clin Neurosci* 2019;63:168-75.
  25. Shankar GM, Lelic N, Gill CM, et al. BRAF alteration status and the histone H3F3A gene K27M mutation segregate spinal cord astrocytoma histology. *Acta Neuropathol* 2016;131:147-50.
  26. Nagaishi M, Nobusawa S, Yokoo H, et al. Genetic mutations in high grade gliomas of the adult spinal cord. *Brain Tumor Pathol* 2016;33:267-9.
  27. Kononov NA, Asyutin DS, Shayhaev EG, et al. Rare cases of IDH1 mutations in spinal cord astrocytomas. *Acta Naturae* 2020;12:70-3.
  28. Malzkorn B, Reifenberger G. Integrated diagnostics of diffuse astrocytic and oligodendroglial tumors. *Pathologie* 2019; 40:9-17.
  29. Ebrahimi A, Skardelly M, Schuhmann MU, et al. High frequency of H3 K27M mutations in adult midline gliomas. *J Cancer Res Clin Oncol* 2019;145:839-50.
  30. Yi S, Choi S, Shin DA, et al. Impact of H3.3 K27M mutation on prognosis and survival of grade IV spinal cord glioma on the basis of new 2016 World Health Organization Classification of the Central Nervous System. *Neurosurgery* 2019;84:1072-81.
  31. Solomon DA, Wood MD, Tihan T, et al. Diffuse midline gliomas with histone H3-K27M mutation: a series of 47 cases assessing the spectrum of morphologic variation and associated genetic alterations. *Brain Pathol* 2016;26:569-80.
  32. Balasubramanian A, Gunjur A, Gan HK, et al. Response to combined BRAF/MEK inhibition in adult BRAF V600E mutant spinal pilocytic astrocytoma. *J Clin Neurosci* 2020;79:269-71.
  33. Horbinski C, Hamilton RL, Nikiforov Y, et al. Association of molecular alterations, including BRAF, with biology and outcome in pilocytic astrocytomas. *Acta Neuropathol* 2010;119:641-9.
  34. Daoud EV, Patel A, Gagan J, et al. Spinal cord pilocytic astrocytoma with FGFR1-TACC1 fusion and anaplastic transformation. *J Neuropathol Exp Neurol* 2021;80:283-5.
  35. Tsutsui T, Arakawa Y, Makino Y, et al. Spinal cord astroblastoma with EWSR1-BEND2 fusion classified as HGNET-MN1 by methylation classification: a case report. *Brain Tumor Pathol* 2021;38:283-9.
  36. Yamasaki K, Nakano Y, Nobusawa S, et al. Spinal cord astroblastoma with an EWSR1-BEND2 fusion classified as a high-grade neuroepithelial tumour with MN1 alteration. *Neuropathol Appl Neurobiol* 2020;46:190-3.
  37. Biczok A, Strubing FL, Eder JM, et al. Molecular diagnostics helps to identify distinct subgroups of spinal astrocytomas. *Acta Neuropathol Commun* 2021;9:119.
  38. Nakamura M, Chiba K, Matsumoto M, et al. Pleomorphic xanthoastrocytoma of the spinal cord. Case report. *J Neurosurg Spine* 2006;5:72-5.
  39. Smith AB, Soderlund KA, Rushing EJ, et al. Radiologic-pathologic correlation of pediatric and adolescent spinal neoplasms: Part 1, Intramedullary spinal neoplasms. *AJR Am J Roentgenol* 2012;198:34-43.
  40. Kang JH, Buckley AF, Nagpal S, et al. A Diffuse leptomeningeal glioneuronal tumor without diffuse leptomeningeal involvement: detailed molecular and clinical characterization. *J Neuropathol Exp Neurol* 2018;77:751-6.
  41. Rodriguez FJ, Schniederjan MJ, Nicolaides T, et al. High rate of concurrent BRAF-KIAA1549 gene fusion and 1p deletion in disseminated oligodendroglioma-like leptomeningeal neoplasms (DOLN). *Acta Neuropathol* 2015;129:609-10.
  42. Rossi S, Rodriguez FJ, Mota RA, et al. Primary leptomeningeal oligodendroglioma with documented progression to anaplasia and t(1;19)(q10;p10) in a child. *Acta Neuropathol* 2009;118:575-7.
  43. Deng MY, Sill M, Chiang J, et al. Molecularly defined diffuse leptomeningeal glioneuronal tumor (DLGNT) comprises two subgroups with distinct clinical and genetic features. *Acta Neuropathol* 2018;136:239-53.
  44. Sali AP, Epari S, Nagaraj TS, et al. Atypical teratoid/rhabdoid tumor: revisiting histomorphology and immunohistochemistry with analysis of cyclin D1 overexpression and MYC amplification. *Int J Surg Pathol* 2021;29:155-64.
  45. Liu YL, Tsai ML, Chen CI, et al. Atypical teratoid/rhabdoid tumor in Taiwan: a nationwide, population-based study. *Cancers (Basel)* 2022;14:668.
  46. Hasselblatt M, Thomas C, Hovestadt V, et al. Poorly differentiated chordoma with SMARCB1/INI1 loss: a distinct molecular entity with dismal prognosis. *Acta Neuropathol* 2016; 132:149-51.
  47. Phi JH. Sacrococcygeal teratoma : a tumor at the center of embryogenesis. *J Korean Neurosurg Soc* 2021;64:406-13.
  48. Imagama S, Ito Z, Ando K, et al. Rapid worsening of symp-

- toms and high cell proliferative activity in intra- and extramedullary spinal hemangioblastoma: a need for earlier surgery. *Global Spine J* 2017;7:6-13.
49. Arumalla K, Deora H, Rao S, et al. Spinal extradural hemangioblastoma: A systematic review of characteristics and outcomes. *J Craniovertebr Junction Spine* 2020;11:254-61.
50. Roy S, Chu A, Trojanowski JQ, et al. D2-40, a novel monoclonal antibody against the M2A antigen as a marker to distinguish hemangioblastomas from renal cell carcinomas. *Acta Neuropathol* 2005;109:497-502.
51. Li J, Jiang XH, Chen AQ, et al. Surgical management of a cervical intramedullary hemangioblastoma presenting with intracystic hemorrhage by hemi-semi-laminectomy via a posterior approach. *J Int Med Res* 2019;47:3458-64.
52. Shankar GM, Taylor-Weiner A, Lelic N, et al. Sporadic hemangioblastomas are characterized by cryptic VHL inactivation. *Acta Neuropathol Commun* 2014;2:167.
53. Sadashivam S, Abraham M, Kesavapisharady K, et al. Long-term outcome and prognostic factors of intramedullary spinal hemangioblastomas. *Neurosurg Rev* 2020;43:169-75.